Originally presented at IPC/JEDEC Global Conference on Lead Free Reliability & Reliability Testing, Boston, MA, April 10-11, 2007. This new version is slightly modified.

Modeling of the JCAA/JG-PP Lead-Free Solder Project Vibration Test Data

Thomas A. Woodrow, Ph.D.
Boeing Phantom Works
Seattle, WA
thomas.a.woodrow@boeing.com

ABSTRACT
Vibration testing was conducted by Boeing Phantom Works (Seattle) for the Joint Council on Aging Aircraft/Joint Group on Pollution Prevention (JCAA/JG-PP) Lead-Free Solder Project. The JCAA/JG-PP Consortium is the first group to test the reliability of lead-free solder joints against the requirements of the aerospace/military community.

A commercially available software package for predicting solder joint lifetimes under vibration was used to model the JG-PP test results. The amount of damage required to fail a BGA at one location on the circuit assembly was used to predict lifetimes for BGA's at other locations on the same circuit assembly. Reasonable agreement between test results and predictions were obtained.

In addition, BGA lifetimes from the accelerated test were extrapolated to field lifetimes. The results indicate that SnPb BGA's will survive much longer than SnAgCu (SAC) BGA's in the same vibration environment.

Key words: Vibration, lead-free solders, reliability, modeling

BACKGROUND
A DoD sponsored consortium was founded in May of 2001 to evaluate lead-free solders and finishes and to determine whether they are suitable for use in high reliability electronics. This consortium was jointly managed by the Joint Council on Aging Aircraft (JCAA) and the Joint Group on Pollution Prevention (JG-PP). The consortium's project was called the JCAA/JG-PP Lead-Free Solder Project and included members from all branches of the Armed Services, Boeing, NASA, Rockwell-Collins, Raytheon, BAE Systems, ACI, Lockheed Martin, Texas Instruments, NCMS, Sandia National Labs, and Marshall Space Flight Center among others.

The consortium wrote a test plan called the Joint Test Protocol (JTP[1]) which described the testing to be done. The testing included vibration, thermal cycling, thermal shock, mechanical shock, combined vibration/thermal cycling, electromigration, SIR, salt fog and humidity.

A test vehicle was designed and the lead-free solders to be tested were chosen. The solder selection process was documented in the Potential Alternatives Report (PAR[2]).

The test vehicle was a six-layer circuit board 14.5 inches wide by 9 inches high by 0.090 inches thick. A break-off coupon populated with chip resistors and chip capacitors was attached to one side of the main test vehicle. With the break-off coupon removed, the main test vehicle was 12.75 in. by 9 inches in size and was populated with 55 components consisting of ceramic leadless chip carriers (CLCC's), plastic leaded chip carriers (PLCC's), TSOP's, TQFP's, BGA's, and PDIP's (Figures 1 and 2). The pads for the CSP's and the hybrids were not populated. The components contained internal wire bonds so that once mounted on the test vehicle, each component would complete an electrical circuit that could be monitored during testing. Failure of a solder joint would cause a break in the electrical circuit that could be detected by an event detector. Each component location on the test vehicles was given a unique reference designator number.

The solder alloys selected for test were:

Sn3.9Ag0.6Cu for reflow and wave soldering (abbreviated as SAC)
Sn3.4Ag1.0Cu3.3Bi for reflow soldering (abbreviated as SACB)
Sn0.7Cu0.05Ni for wave soldering (abbreviated as SnCu)
Sn37Pb for reflow and wave soldering (abbreviated as SnPb)

The SAC alloy was chosen because extensive testing by NEMI suggested it is a viable candidate for use in lead-free commercial electronics. The SACB alloy was chosen because it was the best performer in the large 2001 NCMS

study[3]. The SnCu alloy was chosen because it has been widely used in Asia with good results. Finally, SnPb was included to act as the control alloy.

The test vehicles were divided into two types. The first type (named "Manufactured" test vehicles) were made using a laminate with a high glass transition temperature (Tg of 170 degrees C) and an immersion silver board finish. The "Manufactured" test vehicles were meant to be representative of a printed wiring assembly (PWA) designed for manufacture using lead-free solders and lead-free reflow and wave soldering profiles. Tables 1 and 2 list the components used on the "Manufactured" test vehicles and "Manufactured" control test vehicles; the finish on each component; and the solders used.

The second type (named "Rework" test vehicles) were made using a laminate with a low glass transition temperature (Tg of 140 degrees C) and a tin/lead HASL board finish. The "Rework" test vehicles were meant to be representative of a typical tin/lead PWA that will have to be reworked using lead-free solders in the future. The "Rework" test vehicles were initially built using tin/lead solder and a tin/lead board finish and using typical tin/lead reflow and wave soldering profiles. Selected components on the "Rework" test vehicles were then removed; residual tin/lead solder was cleaned from the pads using solder wick; and new components were attached using a lead-free solder. Components on the "Rework" control test vehicles were reworked with tin/lead solder rather than a lead-free solder. In general, solder wire was used for reworking the components. The BGA's, however, were replaced using flux only and the balls were reflowed using a hot air rework station to form the solder joints. All rework was done at BAE Systems in Irving, TX. Tables 3 and 4 list the components used on the "Rework" test vehicles and "Rework" control test vehicles; the finish on each component; the solders used; and which components were actually reworked.

It is very important to understand that during vibration testing, the vibration environment at a given location on a test vehicle can be very different from the vibration environment at a different location on the same vehicle during the same test. This means that only identical components in identical locations on identical test vehicles can be directly compared. It also implies that the test solder must be used on one set of test vehicles and the control solder on a second set of test vehicles.

Two hundred and five test vehicles were assembled at BAE Systems in Irving, TX. One hundred and nineteen of these test vehicles were "Manufactured" PWA's and eighty six were "Rework" PWA's. Eight components were reworked on each of the "Rework" test vehicles (two BGA's; two TSOP's; two PDIP's; and two TQFP-208's). Thirty of the assembled test vehicles were sent to Boeing in Seattle for vibration testing. These PWA's consisted of 15 "Manufactured" test vehicles and 15 "Rework" test vehicles.

An aluminum fixture was built that could hold up to fifteen test vehicles at one time. Slots were cut into the fixture to accept wedgelocks (torqued to 6 in-lbs, Calmark A260-8.80T2L) that were mounted on both ends of the test vehicles with screws. The wedgelocks were designed with a special locking feature to prevent loosening from vibration.

The electrodynamic shaker used for the test was an Unholtz-Dickie T1000W with a 360 KW amplifier controlled by a Spectral Dynamics 2550B Vibration Controller. The shaker input was controlled by three accelerometers (one on the top of the fixture; one near the bottom of the fixture; and one on the shaker).

The thirty test vehicles were tested in two groups of fifteen vehicles each. The first group of fifteen vehicles were "Manufactured" vehicles and the second group of fifteen were "Rework" vehicles.

Figure 3 shows the fifteen "Manufactured" test vehicles mounted in the test fixture. Figure 4 shows the fixture mounted on a slip table for testing in the z-axis. A calibrated accelerometer was mounted on each test vehicle to record the resonance frequencies and the response of each test vehicle (Figure 2).

Each of the 55 components on the test vehicles were individually monitored using Analysis Tech 256STD Event Detectors (set to a 300 ohm threshold) combined with Labview-based data collection software. The wires connecting the test vehicles to the event detectors had to be glued to the surface of the test vehicles (Figure 2) to prevent them from flexing and breaking at the solder joints during the vibration test. In addition, the wire bundles from the test vehicles were firmly clamped to the fixture in order to prevent flexing and breaking of the wires. All wire bundles were covered with a grounded metallic shield to prevent electrical noise from the shaker from interfering with the event detectors.

Each group of test vehicles was subjected to the vibration levels shown in Figure 5 and Table 5. The test consisted of one hour of vibration at 9.9 Grms in the y-axis, followed by one hour of vibration at 9.9 Grms in the x-axis, followed by one hour of vibration at 9.9 Grms in the z-axis. Then the test vehicles were subjected to additional step stress vibration in the z-axis only, starting with one hour of vibration at 12.0 Grms. The vibration levels were then increased in 2.0 Grms increments, shaking at each level in the z-axis for one hour until completion of the 20.0 Grms run. A final one hour run at 28.0 Grms completed the test.

Figure 6 shows the shaker input into the test vehicles and Figure 7 shows the typical response of a "Manufactured" test vehicle (both during a 14.0 Grms run). Note that the response of the test vehicle differs greatly from the input PSD spectrum with the major test vehicle resonances occurring at 72 Hz (the first mode, Figure 8) and 411 Hz.

Figure 9 shows the displacement of a test vehicle vs. frequency (from accelerometer data during a 1 G sine sweep of a "Manufactured" test vehicle in the z-axis). This illustrates that the most displacement (and therefore the most solder joint damage) is associated with the first mode (at 72 Hz).

The time to failure (in minutes) for each component on a typical "Manufactured" test vehicle is shown in Figure 10. As noted earlier, the random vibration spectrum was increased in amplitude every 60 minutes and the total length of the test (in the z-axis) was 420 minutes. Only the z-axis test minutes are shown since shaking in the x- and y-axes do little damage. Any component that did not fail during the test is shown as having survived 420+ minutes. Note that the components that failed first were those on the centerline of the vehicle and those down the sides of the vehicle (near the wedgelocks). Therefore, the components that failed first coincide with the regions of highest curvature induced by the first bending mode (see Figure 8).

A test report documenting the details of the vibration testing and all of the test results was written[4] and can be found online at http://acqp2.nasa.gov/projects/LeadFreeSolderTestingForHighReliability_Proj1.html.

OBJECTIVE AND APPROACH

The objective of this ongoing study is to use the JCAA/JG-PP Lead-Free Solder Vibration Test results to validate solder joint lifetime prediction models available in the public domain. These models are needed in order to predict solder joint lifetimes under field conditions. Accelerated vibration test data (such as the JCAA/JG-PP data) is needed in order to validate the prediction accuracy of the available models.

CirVibe, Inc. of Plymouth, MN markets a finite element-based software package for predicting solder joint failures on circuit board assemblies under vibration. The results from the JCAA/JG-PP Vibration Test were used to evaluate the predictive capabilities of this software.

The general steps required for an analysis using CirVibe software are as follows:

1. The circuit board design must be created within the software. If the original CAD files are available, they can be imported into the software which greatly facilitates the process (see Figure 11).

2. Material properties must be assigned to each component and the solder used.

3. The fixturing holding the circuit board is then defined (e.g., wedgelocks on two sides of the circuit board).

4. If modal data for the circuit board is available from accelerometer measurements, the data is entered. To get good results, the transmissibilities and frequencies of the first three modes are required (transmissibility is a measure of how much of the energy applied to the electrodynamic shaker actually gets into the circuit board at a given resonance frequency). These parameters are best obtained by measuring them using an actual circuit board mounted on an electrodynamic shaker.

5. The input spectrum (PSD or power spectral density spectrum) is then defined.

6. The material properties of the circuit board are then defined.

7. The analysis is run and the amount of damage accumulated per minute by the solder joints on each component are calculated and tabulated. The damage numbers are good indicators of which components are at risk for early failure.

The software requires the slope of the S-N plot (stress vs. cycles to failure) for the solder in order to calculate the damage accumulation rates. The S-N slope (-1/b) used for SnPb solder was -0.10003[5]. The S-N plot slope used for the analyses of the SAC solder joints described in this report was -0.1106[6]. It should be noted that the S-N plot for SAC has not been definitively determined and that this is the best number available at this time.

In order to predict how long a component type will survive at various positions on a circuit assembly, the amount of damage required to fail that component type must be known. The amount of damage required to fail a component is simply the time required to fail the component (from test) times the damage accumulation rate for that component (provided by the software). Once the amount of damage required to fail a component at one location on the circuit assembly is known, then the calculated damage accumulation rates for other components of the same type on the same circuit assembly can be used to predict when those other components will fail. In theory, the damage required to fail a component on one circuit assembly design can also be used to predict how long that same component type would survive on a different circuit assembly design. Error can be introduced into the predictions, however, if the initial damage number used for the predictions is not representative of the average amount of damage required to fail that component type.

For example, the times to failure for the BGA's on JG-PP Test Vehicle 7 were predicted by using the calculated damage accumulation rates for each BGA and the amount of damage required to fail that type of BGA. The first BGA to fail on that test vehicle was U4 which failed at 61 minutes into the test. The amount of damage accumulated per minute by U4 (at 9.9 Grms) was 0.003448 damage units.

Since a step stress test was used, all test minutes have to be converted into equivalent life minutes before the calculation of accumulated damage can be done (in this case, equivalent life minutes are the number of minutes the component would have lasted if the test had been run at a constant 9.9 Grms). This is required because the minutes spent at the higher steps are much more damaging than the minutes spent at 9.9 Grms. The equivalent life minutes (at 9.9 Grms) are calculated by multiplying the minutes spent at each step by an acceleration factor for each step and then summing the products (see Equation 1).

Eq. 1 Equivalent Life Minutes (at 9.9 Grms) = Σ(Life in Minutes at Step n)(Acceleration Factor for Step n)

The acceleration factor for each step was calculated using Equation 2. This equation is valid if the first resonance frequency (f_n) is the same for each step. The acceleration factors calculated for Test Vehicles 5 and 7 are shown in Table 6. The acceleration factors are not the same for each test vehicle due to normal variations in the responses of the vehicles during the vibration test.

Eq. 2

$$\text{Acceleration Factor} = \frac{\left(\sqrt{PSD_2}\sqrt{Q_2}\right)^b}{\left(\sqrt{PSD_1}\sqrt{Q_1}\right)^b}$$

b = solder fatigue exponent (negative inverse of the slope of the solder S-N plot)
PSD_1 = input PSD in G^2/Hz for the first mode resonance at the 9.9 Grms level
PSD_2 = input PSD in G^2/Hz for the first mode resonance at step stress level n
Q_1 = transmissibility for the first mode resonance at the 9.9 Grms level
Q_2 = transmissibility for the first mode resonance at step stress level n

The damage accumulation rate for BGA U4 on Test Vehicle 7 (0.003448 damage units/min) times the equivalent life minutes actually required to fail U4 (65.74 min) equals the amount of damage required to fail U4 (i.e., 0.2267 damage units). To predict the survival times for the other BGA's on Test Vehicle 7, 0.2267 (the amount of damage required to fail that type of BGA) was divided by the damage accumulation rate for each BGA to yield the

equivalent life minutes (i.e., the survival times for the BGA's). The survival times in equivalent life minutes were then converted into test minutes for comparison.

In addition, a test lifetime can be extrapolated to a field lifetime for any field condition. In this paper, Equation 3 was used to predict field lifetimes by extrapolation of the JG-PP Vibration Test data. The test data used for the extrapolations was from test vehicles that had similar transmissibilities so that fair comparisons could be made. In addition, it was assumed that the shape of the test PSD and the field PSD were the same. Again, the minutes that the solder joints survived at each test level had to be converted into the number of minutes that they would have survived if the test had been run at a constant 9.9 Grms (i.e., equivalent life minutes).

Eq. 3

$$\text{Field Lifetime} = \frac{(\text{9.9 Grms})^{b}}{(\text{Grms in the Field})^{b}} \bullet \text{Equivalent Life Minutes (at 9.9 Grms)}$$

b = solder fatigue exponent (negative inverse of the slope of the solder S-N plot)
Equivalent Life Minutes (at 9.9 Grms) = Σ(Life in Minutes at Step n)(Acceleration Factor for Step n)

RESULTS AND DISCUSSION

The life predictions performed at Boeing for SnPb and SAC BGA's are shown in Tables 7 through 11. CirVibe software was used to calculate the damage accumulated by BGA solder joints on selected JG-PP test vehicles. The Q values (transmissibilities) used for the calculations are shown and they were derived from accelerometer measurements taken during a 1 G sine sweep of each test vehicle. The amount of damage accumulated by a single BGA (usually the first to fail) was used to calculate the lifetimes of the other BGA's on each test vehicle. The life predictions were then compared to the actual test results in tabular and graphic formats. All times are presented as test minutes and not as equivalent life minutes. In addition, the predicted BGA lifetimes at two additional vibration levels are shown (at 5 Grms and at 3 Grms). These extrapolations were made using the actual test lifetimes and not the predicted test lifetimes. The vibration levels chosen are much less severe then those used for the actual JG-PP Vibration Test although the shape of the PSD input from the test was retained for the extrapolations. The tables also show which modes caused the most damage to each BGA.

The frequencies of the first three modes as predicted by the software are shown in Figure 12. The predictions of 72, 101 and 202 Hz compare well to the actual measured frequencies of 72, 101 and 210 Hz.

Table 7 shows the lifetimes (from test and predicted) for the ten BGA's on Test Vehicle 5. These BGA's had SnPb balls and were assembled with SnPb solder paste. Eight of the ten predictions appear to be a reasonable match to the actual test data. Cirvibe, Inc. felt that the lifetime of U21 was not correctly predicted because it is in a region that was affected by both Mode 1 and Mode 2. The software can assign more damage to a component when two modes dominate and the predicted lifetime is sometimes shorter than would be the case if only one mode dominated. Cirvibe, Inc. felt that the lifetime of U55 was not correctly predicted because it was in a region of very high curvature (near the wedgelocks) which requires a higher level finite element model than that used by CirVibe.

The predicted lifetimes of the SnPb BGA's at vibration levels of 5 and 3 Grms are also shown. At the 3 Grms level, the extrapolations show that none of the BGA's will fail during the first ten years of service. Milder vibration environments will further extend their lifetimes. At the 5 Grms level, however, most of the BGA's are at risk. It is important to again note that the exact position of a component on the circuit board plays a huge role in how long a component will last as is demonstrated by the large variation in lifetimes expected for the ten BGA's.

Table 8 shows the predicted lifetimes of the ten SnPb BGA's on Test Vehicle 7. Again, reasonable agreement between predicted and test lifetimes was obtained especially for those BGA's that failed early. These are the most important BGA's because they are the ones that will fail first in the field. The ability to correctly predict which components are the weakest will allow design changes to be made early in the design process.

Table 9 shows the predicted lifetimes of the ten SnPb BGA's on Test Vehicle 8.

Tables 10 and 11 show the predicted lifetimes of the SAC BGA's on Test Vehicles 75 and 77, respectively. Good agreement between test and predicted lifetimes was obtained. The predicted lifetimes of the BGA's at vibration

levels of 5 and 3 Grms are shown. It should be noted that some of the BGA's are at risk of failing within the first year of service at the 3 Grms level.

The best lifetime predictions are only possible when the transmissibilities of the first three modes are accurately known. In the JG-PP test, only one accelerometer was placed on each test vehicle. One accelerometer can not be expected to accurately measure the transmissibilites for every mode. Better agreement between test and prediction might have been obtained if multiple accelerometers had been placed on each test vehicle at the points of maximum displacement for each of the first three modes.

Table 12 compares the predicted lifetimes for SnPb and SAC BGA's assuming they were exposed to a constant 3 Grms until failure (0.0062 G^2/Hz input into the first resonance). The predictions were obtained by extrapolation of accelerated JG-PP test data using Equation 3. The test data used for the extrapolations was from test vehicles that had similar transmissibilities so that fair comparisons could be made. The comparisons reveal that the predicted SnPb solder joint lifetimes are much longer than those predicted for SAC in the same vibration environment (approximately 20 times longer for U4). This could be cause for concern for some Pb-free electronics depending on their use environments. Further test and analysis should be done before SAC is widely accepted for use in high reliability electronics.

SUMMARY

A commercially available software package (CirVibe) for doing solder joint lifetime predictions under vibration was used to model test data from the JCAA/JG-PP Lead-Free Solder Project. This software can predict which components will fail first on a circuit assembly and if the amount of damage required to fail a component type is known (from test) then actual times to failure can be predicted for that component type regardless of its position on a circuit assembly. Extrapolations of actual BGA test lifetimes to a 3 Grms field condition revealed that SnPb BGA's will outlast SAC BGA's by a factor of approximately 20 times. This indicates that the use of SAC BGA's in high reliability electronics could be problematic for some vibration environments.

ACKNOWLEDGEMENTS

Thanks to John Starr of CirVibe, Inc. for numerous and invaluable discussions concerning vibration analysis. Also, a special thanks to the Boeing MS&MT Thrust for funding this study.

REFERENCES

1. J-01-EM-026-P1, "Draft Joint Test Protocol for Validation of Alternatives to Eutectic Tin-Lead Solders used in Manufacturing and Rework of Printed Wiring Assemblies", Joint Group on Pollution Prevention (JG-PP), February 14, 2003 (revised April 2004).

2. "Potential Alternatives Report for Validation of Alternatives to Eutectic Tin-Lead Solders used in Electronics Manufacturing and Repair, Final", Contract No. DAAE30-98-C-1050, Task 272, Concurrent Technologies Corporation, Johnstown, PA, May 27, 2003.

3. NCMS Report 0096RE01, "Lead-Free, High-Temperature Fatigue-Resistant Solder, Final Report", National Center for Manufacturing Sciences, August 2001.

4. T. Woodrow, "JCAA/JG-PP Lead-Free Solder Project: Vibration Test", Boeing Electronics Materials and Processes Report – 582, Revision A, January 9, 2006 (available at http://acqp2.nasa.gov/JTR.htm).

5. Steinberg, Dave S., *Vibration Analysis for Electronic Equipment*, 2nd Edition, John Wiley & Sons, Inc., 1988.

6. Zhou, YuXun; Dasgupta, Abhijit, "Vibration Durability Investigation for SAC and SnPb Solder: Based on JCAA/JG-PP Lead-Free Solder Project Test Results", Second Draft, CALCE (U of Maryland), October 27, 2006 (available at http://acqp2.nasa.gov/JTR.htm).

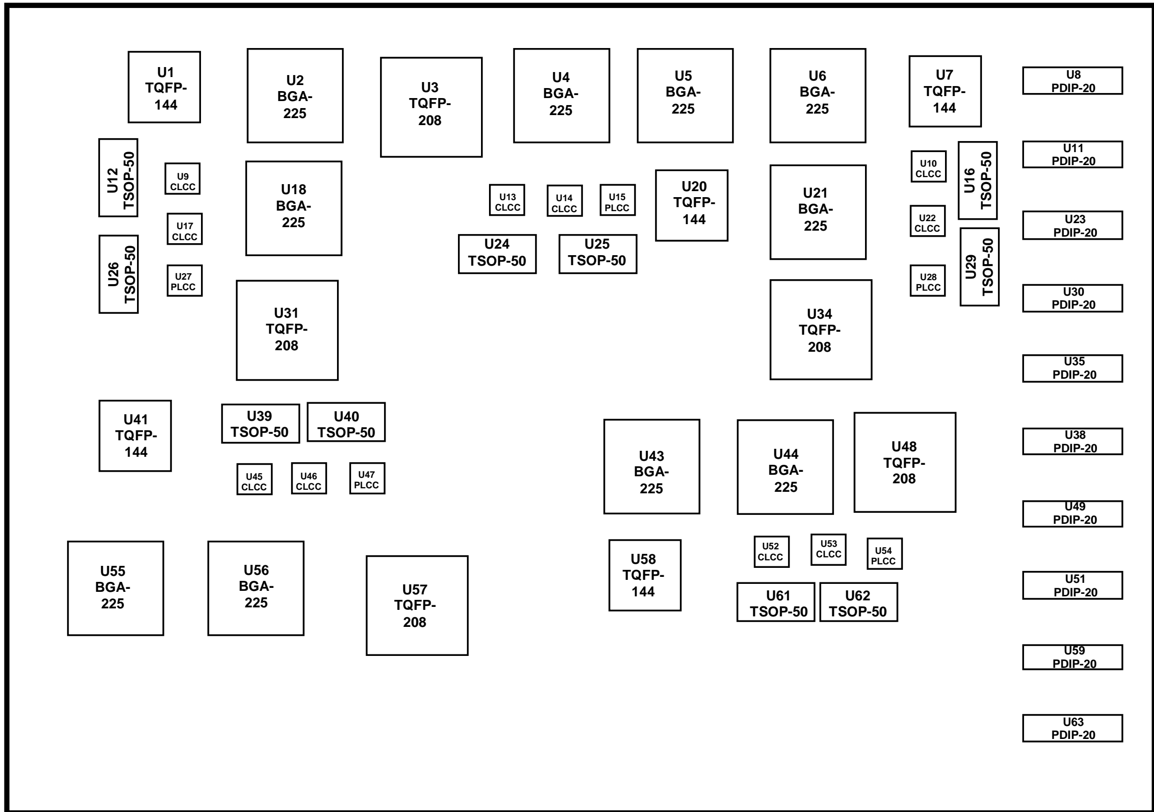

Figure 1. Main Test Vehicle Schematic

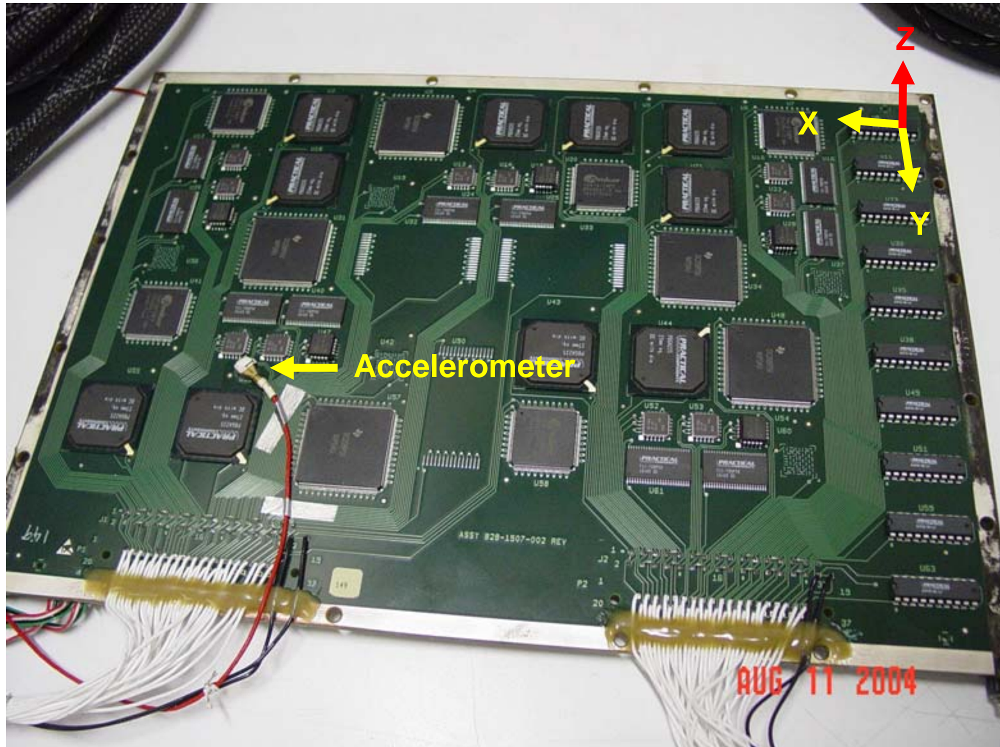

Figure 2. Test Vehicle showing Accelerometer Placement

Table 1. Test Vehicle Key ("Manufactured" Test Vehicles – Controls)

Test Vehicle ID Numbers: 5 through 9

Reference Designator	Component	Component Finish	Reflow Solder Alloy	Wave Solder Alloy (DIP's only)
U1	TQFP-144	Sn	SnPb	
U2	BGA-225	SnPb	SnPb	
U3	TQFP-208	NiPdAu	SnPb	
U4	BGA-225	SnPb	SnPb	
U5	BGA-225	SnPb	SnPb	
U6	BGA-225	SnPb	SnPb	
U7	TQFP-144	Sn	SnPb	
U8	PDIP-20	NiPdAu		SnPb
U9	CLCC-20	SnPb	SnPb	
U10	CLCC-20	SnPb	SnPb	
U11	PDIP-20	Sn		SnPb
U12	TSOP-50	SnPb	SnPb	
U13	CLCC-20	SnPb	SnPb	
U14	CLCC-20	SnPb	SnPb	
U15	PLCC-20	Sn	SnPb	
U16	TSOP-50	SnPb	SnPb	
U17	CLCC-20	SnPb	SnPb	
U18	BGA-225	SnPb	SnPb	
U19	CSP-100	SnPb	SnPb	
U20	TQFP-144	Sn	SnPb	
U21	BGA-225	SnPb	SnPb	
U22	CLCC-20	SnPb	SnPb	
U23	PDIP-20	NiPdAu		SnPb
U24	TSOP-50	SnPb	SnPb	
U25	TSOP-50	SnPb	SnPb	
U26	TSOP-50	SnPb	SnPb	
U27	PLCC-20	Sn	SnPb	
U28	PLCC-20	Sn	SnPb	
U29	TSOP-50	SnPb	SnPb	
U30	PDIP-20	Sn		SnPb
U31	TQFP-208	NiPdAu	SnPb	
U32	Hybrid-30	SnPb	SnPb	
U33	Hybrid-30	SnPb	SnPb	
U34	TQFP-208	NiPdAu	SnPb	
U35	PDIP-20	NiPdAu		SnPb
U36	CSP-100	SnPb	SnPb	
U37	CSP-100	SnPb	SnPb	
U38	PDIP-20	Sn		SnPb
U39	TSOP-50	SnPb	SnPb	
U40	TSOP-50	SnPb	SnPb	
U41	TQFP-144	Sn	SnPb	
U42	CSP-100	SnPb	SnPb	
U43	BGA-225	SnPb	SnPb	
U44	BGA-225	SnPb	SnPb	
U45	CLCC-20	SnPb	SnPb	
U46	CLCC-20	SnPb	SnPb	
U47	PLCC-20	Sn	SnPb	
U48	TQFP-208	NiPdAu	SnPb	
U49	PDIP-20	NiPdAu		SnPb
U50	Hybrid-30	SnPb	SnPb	
U51	PDIP-20	Sn		SnPb
U52	CLCC-20	SnPb	SnPb	
U53	CLCC-20	SnPb	SnPb	
U54	PLCC-20	Sn	SnPb	
U55	BGA-225	SnPb	SnPb	
U56	BGA-225	SnPb	SnPb	
U57	TQFP-208	NiPdAu	SnPb	
U58	TQFP-144	Sn	SnPb	
U59	PDIP-20	NiPdAu		SnPb
U60	CSP-100	SnPb	SnPb	
U61	TSOP-50	SnPb	SnPb	
U62	TSOP-50	SnPb	SnPb	
U63	PDIP-20	Sn		SnPb

Hybrids and CSPs were left off of the test vehicles.

Table 2. Test Vehicle Key ("Manufactured" Test Vehicles)

		Test Vehicle ID Numbers: 75 through 79			Test Vehicle ID Numbers: 114 through 118		
Reference Designator	Component	Component Finish	Reflow Solder Alloy	Wave Solder Alloy (DIP's only)	Component Finish	Reflow Solder Alloy	Wave Solder Alloy (DIP's only)
U1	TQFP-144	Sn	Sn3.9Ag0.6Cu		Sn	Sn3.4Ag1Cu3.3Bi	
U2	BGA-225	SnPb	Sn3.9Ag0.6Cu		SnPb	Sn3.4Ag1Cu3.3Bi	
U3	TQFP-208	NiPdAu	Sn3.9Ag0.6Cu		NiPdAu	Sn3.4Ag1Cu3.3Bi	
U4	BGA-225	SnAgCu	Sn3.9Ag0.6Cu		SnAgCu	Sn3.4Ag1Cu3.3Bi	
U5	BGA-225	SnPb	Sn3.9Ag0.6Cu		SnPb	Sn3.4Ag1Cu3.3Bi	
U6	BGA-225	SnAgCu	Sn3.9Ag0.6Cu		SnAgCu	Sn3.4Ag1Cu3.3Bi	
U7	TQFP-144	Sn	Sn3.9Ag0.6Cu		Sn	Sn3.4Ag1Cu3.3Bi	
U8	PDIP-20	NiPdAu		Sn3.9Ag0.6Cu	NiPdAu		Sn0.7Cu0.05Ni
U9	CLCC-20	SnPb	Sn3.9Ag0.6Cu		SnPb	Sn3.4Ag1Cu3.3Bi	
U10	CLCC-20	Sn3.9Ag0.6Cu	Sn3.9Ag0.6Cu		Sn3.4Ag1Cu3.3Bi	Sn3.4Ag1Cu3.3Bi	
U11	PDIP-20	Sn		Sn3.9Ag0.6Cu	Sn		Sn0.7Cu0.05Ni
U12	TSOP-50	SnCu	Sn3.9Ag0.6Cu		SnCu	Sn3.4Ag1Cu3.3Bi	
U13	CLCC-20	SnPb	Sn3.9Ag0.6Cu		SnPb	Sn3.4Ag1Cu3.3Bi	
U14	CLCC-20	Sn3.9Ag0.6Cu	Sn3.9Ag0.6Cu		Sn3.4Ag1Cu3.3Bi	Sn3.4Ag1Cu3.3Bi	
U15	PLCC-20	Sn	Sn3.9Ag0.6Cu		Sn	Sn3.4Ag1Cu3.3Bi	
U16	TSOP-50	SnPb	Sn3.9Ag0.6Cu		SnPb	Sn3.4Ag1Cu3.3Bi	
U17	CLCC-20	Sn3.9Ag0.6Cu	Sn3.9Ag0.6Cu		Sn3.4Ag1Cu3.3Bi	Sn3.4Ag1Cu3.3Bi	
U18	BGA-225	SnAgCu	Sn3.9Ag0.6Cu		SnAgCu	Sn3.4Ag1Cu3.3Bi	
U19	CSP-100	SnAgCu	Sn3.9Ag0.6Cu		SnAgCu	Sn3.4Ag1Cu3.3Bi	
U20	TQFP-144	Sn	Sn3.9Ag0.6Cu		Sn	Sn3.4Ag1Cu3.3Bi	
U21	BGA-225	SnPb	Sn3.9Ag0.6Cu		SnPb	Sn3.4Ag1Cu3.3Bi	
U22	CLCC-20	SnPb	Sn3.9Ag0.6Cu		SnPb	Sn3.4Ag1Cu3.3Bi	
U23	PDIP-20	NiPdAu		Sn3.9Ag0.6Cu	NiPdAu		Sn0.7Cu0.05Ni
U24	TSOP-50	SnPb	Sn3.9Ag0.6Cu		SnPb	Sn3.4Ag1Cu3.3Bi	
U25	TSOP-50	SnCu	Sn3.9Ag0.6Cu		SnCu	Sn3.4Ag1Cu3.3Bi	
U26	TSOP-50	SnPb	Sn3.9Ag0.6Cu		SnPb	Sn3.4Ag1Cu3.3Bi	
U27	PLCC-20	Sn	Sn3.9Ag0.6Cu		Sn	Sn3.4Ag1Cu3.3Bi	
U28	PLCC-20	Sn	Sn3.9Ag0.6Cu		Sn	Sn3.4Ag1Cu3.3Bi	
U29	TSOP-50	SnCu	Sn3.9Ag0.6Cu		SnCu	Sn3.4Ag1Cu3.3Bi	
U30	PDIP-20	Sn		Sn3.9Ag0.6Cu	Sn		Sn0.7Cu0.05Ni
U31	TQFP-208	NiPdAu	Sn3.9Ag0.6Cu		NiPdAu	Sn3.4Ag1Cu3.3Bi	
U32	Hybrid-30	Sn3.9Ag0.6Cu	Sn3.9Ag0.6Cu		Sn3.4Ag1Cu3.3Bi	Sn3.4Ag1Cu3.3Bi	
U33	Hybrid-30	Sn3.9Ag0.6Cu	Sn3.9Ag0.6Cu		Sn3.4Ag1Cu3.3Bi	Sn3.4Ag1Cu3.3Bi	
U34	TQFP-208	NiPdAu	Sn3.9Ag0.6Cu		NiPdAu	Sn3.4Ag1Cu3.3Bi	
U35	PDIP-20	NiPdAu		Sn3.9Ag0.6Cu	NiPdAu		Sn0.7Cu0.05Ni
U36	CSP-100	SnAgCu	Sn3.9Ag0.6Cu		SnAgCu	Sn3.4Ag1Cu3.3Bi	
U37	CSP-100	SnAgCu	Sn3.9Ag0.6Cu		SnAgCu	Sn3.4Ag1Cu3.3Bi	
U38	PDIP-20	Sn		Sn3.9Ag0.6Cu	Sn		Sn0.7Cu0.05Ni
U39	TSOP-50	SnCu	Sn3.9Ag0.6Cu		SnCu	Sn3.4Ag1Cu3.3Bi	
U40	TSOP-50	SnPb	Sn3.9Ag0.6Cu		SnPb	Sn3.4Ag1Cu3.3Bi	
U41	TQFP-144	Sn	Sn3.9Ag0.6Cu		Sn	Sn3.4Ag1Cu3.3Bi	
U42	CSP-100	SnAgCu	Sn3.9Ag0.6Cu		SnAgCu	Sn3.4Ag1Cu3.3Bi	
U43	BGA-225	SnAgCu	Sn3.9Ag0.6Cu		SnAgCu	Sn3.4Ag1Cu3.3Bi	
U44	BGA-225	SnPb	Sn3.9Ag0.6Cu		SnPb	Sn3.4Ag1Cu3.3Bi	
U45	CLCC-20	Sn3.9Ag0.6Cu	Sn3.9Ag0.6Cu		Sn3.4Ag1Cu3.3Bi	Sn3.4Ag1Cu3.3Bi	
U46	CLCC-20	SnPb	Sn3.9Ag0.6Cu		SnPb	Sn3.4Ag1Cu3.3Bi	
U47	PLCC-20	Sn	Sn3.9Ag0.6Cu		Sn	Sn3.4Ag1Cu3.3Bi	
U48	TQFP-208	NiPdAu	Sn3.9Ag0.6Cu		NiPdAu	Sn3.4Ag1Cu3.3Bi	
U49	PDIP-20	NiPdAu		Sn3.9Ag0.6Cu	NiPdAu		Sn0.7Cu0.05Ni
U50	Hybrid-30	Sn3.9Ag0.6Cu	Sn3.9Ag0.6Cu		Sn3.4Ag1Cu3.3Bi	Sn3.4Ag1Cu3.3Bi	
U51	PDIP-20	Sn		Sn3.9Ag0.6Cu	Sn		Sn0.7Cu0.05Ni
U52	CLCC-20	Sn3.9Ag0.6Cu	Sn3.9Ag0.6Cu		Sn3.4Ag1Cu3.3Bi	Sn3.4Ag1Cu3.3Bi	
U53	CLCC-20	SnPb	Sn3.9Ag0.6Cu		SnPb	Sn3.4Ag1Cu3.3Bi	
U54	PLCC-20	Sn	Sn3.9Ag0.6Cu		Sn	Sn3.4Ag1Cu3.3Bi	
U55	BGA-225	SnAgCu	Sn3.9Ag0.6Cu		SnAgCu	Sn3.4Ag1Cu3.3Bi	
U56	BGA-225	SnPb	Sn3.9Ag0.6Cu		SnPb	Sn3.4Ag1Cu3.3Bi	
U57	TQFP-208	NiPdAu	Sn3.9Ag0.6Cu		NiPdAu	Sn3.4Ag1Cu3.3Bi	
U58	TQFP-144	Sn	Sn3.9Ag0.6Cu		Sn	Sn3.4Ag1Cu3.3Bi	
U59	PDIP-20	NiPdAu		Sn3.9Ag0.6Cu	NiPdAu		Sn0.7Cu0.05Ni
U60	CSP-100	SnAgCu	Sn3.9Ag0.6Cu		SnAgCu	Sn3.4Ag1Cu3.3Bi	
U61	TSOP-50	SnCu	Sn3.9Ag0.6Cu		SnCu	Sn3.4Ag1Cu3.3Bi	
U62	TSOP-50	SnPb	Sn3.9Ag0.6Cu		SnPb	Sn3.4Ag1Cu3.3Bi	
U63	PDIP-20	Sn		Sn3.9Ag0.6Cu	Sn		Sn0.7Cu0.05Ni

Hybrids and CSPs were left off of the test vehicles.
SnAgCu BGA balls were Sn4.0Ag0.5Cu.

Table 3. Test Vehicle Key ("Rework" Test Vehicles – Controls)

Test Vehicle ID Numbers: 43, 46, 47, 49, 50

Reference Designator	Component	Component Finish (Before Rework)	Reflow Solder Alloy (Before Rework)	Wave Solder Alloy (Before Rework)	Component Finish (After Rework)	Rework Solder Alloy
U1	TQFP-144	Sn	SnPb			
U2	BGA-225	SnPb	SnPb			
U3	TQFP-208	NiPdAu	SnPb		NiPdAu	SnPb
U4	BGA-225	SnPb	SnPb		SnPb	SnPb
U5	BGA-225	SnPb	SnPb			
U6	BGA-225	SnPb	SnPb			
U7	TQFP-144	Sn	SnPb			
U8	PDIP-20	NiPdAu		SnPb		
U9	CLCC-20	SnPb	SnPb			
U10	CLCC-20	SnPb	SnPb			
U11	PDIP-20	Sn		SnPb		
U12	TSOP-50	SnPb	SnPb		SnPb	SnPb
U13	CLCC-20	SnPb	SnPb			
U14	CLCC-20	SnPb	SnPb			
U15	PLCC-20	Sn	SnPb			
U16	TSOP-50	SnPb	SnPb			
U17	CLCC-20	SnPb	SnPb			
U18	BGA-225	SnPb	SnPb		SnPb	SnPb
U19	CSP-100	SnPb	SnPb			
U20	TQFP-144	Sn	SnPb			
U21	BGA-225	SnPb	SnPb			
U22	CLCC-20	SnPb	SnPb			
U23	PDIP-20	NiPdAu		SnPb	NiPdAu	SnPb
U24	TSOP-50	SnPb	SnPb			
U25	TSOP-50	SnPb	SnPb		SnPb	SnPb
U26	TSOP-50	SnPb	SnPb			
U27	PLCC-20	Sn	SnPb			
U28	PLCC-20	Sn	SnPb			
U29	TSOP-50	SnPb	SnPb			
U30	PDIP-20	Sn		SnPb		
U31	TQFP-208	NiPdAu	SnPb			
U32	Hybrid-30	SnPb	SnPb			
U33	Hybrid-30	SnPb	SnPb			
U34	TQFP-208	NiPdAu	SnPb			
U35	PDIP-20	NiPdAu		SnPb		
U36	CSP-100	SnPb	SnPb			
U37	CSP-100	SnPb	SnPb			
U38	PDIP-20	Sn		SnPb		
U39	TSOP-50	SnPb	SnPb			
U40	TSOP-50	SnPb	SnPb			
U41	TQFP-144	Sn	SnPb			
U42	CSP-100	SnPb	SnPb			
U43	BGA-225	SnPb	SnPb			
U44	BGA-225	SnPb	SnPb			
U45	CLCC-20	SnPb	SnPb			
U46	CLCC-20	SnPb	SnPb			
U47	PLCC-20	Sn	SnPb			
U48	TQFP-208	NiPdAu	SnPb			
U49	PDIP-20	NiPdAu		SnPb		
U50	Hybrid-30	SnPb	SnPb			
U51	PDIP-20	Sn		SnPb		
U52	CLCC-20	SnPb	SnPb			
U53	CLCC-20	SnPb	SnPb			
U54	PLCC-20	Sn	SnPb			
U55	BGA-225	SnPb	SnPb			
U56	BGA-225	SnPb	SnPb			
U57	TQFP-208	NiPdAu	SnPb		NiPdAu	SnPb
U58	TQFP-144	Sn	SnPb			
U59	PDIP-20	NiPdAu		SnPb	NiPdAu	SnPb
U60	CSP-100	SnPb	SnPb			
U61	TSOP-50	SnPb	SnPb			
U62	TSOP-50	SnPb	SnPb			
U63	PDIP-20	Sn		SnPb		

Reworked components are shown in red.
Hybrids and CSPs were left off of the test vehicles.

Originally presented at IPC/JEDEC Global Conference on Lead Free Reliability & Reliability Testing, Boston, MA, April 10-11, 2007. This new version is slightly modified.

Table 4. Test Vehicle Key ("Rework" Test Vehicles)

				Test Vehicle ID Numbers: 153 through 157			Test Vehicle ID Numbers: 180, 182 through 185		
Reference Designator	**Component**	**Reflow Solder Alloy (Before Rework)**	**Wave Solder Alloy (Before Rework)**	**Component Finish (Before Rework)**	**Component Finish (After Rework)**	**Rework Solder Alloy**	**Component Finish (Before Rework)**	**Component Finish (After Rework)**	**Rework Solder Alloy**
U1	TQFP-144	SnPb		Sn			Sn		
U2	BGA-225	SnPb		SnAgCu			SnAgCu		
U3	TQFP-208	SnPb		NiPdAu	NiPdAu	Sn3.9Ag0.6Cu	NiPdAu	NiPdAu	Sn3.4Ag1Cu3.3Bi
U4	BGA-225	SnPb		SnPb	SnAgCu	flux only	SnPb	SnAgCu	flux only
U5	BGA-225	SnPb		SnAgCu			SnAgCu		
U6	BGA-225	SnPb		SnAgCu			SnAgCu		
U7	TQFP-144	SnPb		Sn			Sn		
U8	PDIP-20		SnPb	NiPdAu			NiPdAu		
U9	CLCC-20	SnPb		Sn3.9Ag0.6Cu			Sn3.4Ag1Cu3.3Bi		
U10	CLCC-20	SnPb		Sn3.9Ag0.6Cu			Sn3.4Ag1Cu3.3Bi		
U11	PDIP-20		SnPb	Sn			Sn		
U12	TSOP-50	SnPb		SnPb	SnCu	Sn3.9Ag0.6Cu	SnPb	SnCu	Sn3.4Ag1Cu3.3Bi
U13	CLCC-20	SnPb		Sn3.9Ag0.6Cu			Sn3.4Ag1Cu3.3Bi		
U14	CLCC-20	SnPb		Sn3.9Ag0.6Cu			Sn3.4Ag1Cu3.3Bi		
U15	PLCC-20	SnPb		Sn			Sn		
U16	TSOP-50	SnPb		SnCu			SnCu		
U17	CLCC-20	SnPb		Sn3.9Ag0.6Cu			Sn3.4Ag1Cu3.3Bi		
U18	BGA-225	SnPb		SnPb	SnAgCu	flux only	SnPb	SnAgCu	flux only
U19	CSP-100	SnPb		SnAgCu			SnAgCu		
U20	TQFP-144	SnPb		Sn			Sn		
U21	BGA-225	SnPb		SnAgCu			SnAgCu		
U22	CLCC-20	SnPb		Sn3.9Ag0.6Cu			Sn3.4Ag1Cu3.3Bi		
U23	PDIP-20		SnPb	NiPdAu	NiPdAu	Sn3.9Ag0.6Cu	NiPdAu	NiPdAu	Sn0.7Cu0.05Ni
U24	TSOP-50	SnPb		SnCu			SnCu		
U25	TSOP-50	SnPb		SnPb	SnCu	Sn3.9Ag0.6Cu	SnPb	SnCu	Sn3.4Ag1Cu3.3Bi
U26	TSOP-50	SnPb		SnCu			SnCu		
U27	PLCC-20	SnPb		Sn			Sn		
U28	PLCC-20	SnPb		Sn			Sn		
U29	TSOP-50	SnPb		SnCu			SnCu		
U30	PDIP-20		SnPb	Sn			Sn		
U31	TQFP-208	SnPb		NiPdAu			NiPdAu		
U32	Hybrid-30	SnPb		Sn3.9Ag0.6Cu			Sn3.4Ag1Cu3.3Bi		
U33	Hybrid-30	SnPb		Sn3.9Ag0.6Cu			Sn3.4Ag1Cu3.3Bi		
U34	TQFP-208	SnPb		NiPdAu			NiPdAu		
U35	PDIP-20		SnPb	NiPdAu			NiPdAu		
U36	CSP-100	SnPb		SnAgCu			SnAgCu		
U37	CSP-100	SnPb		SnAgCu			SnAgCu		
U38	PDIP-20		SnPb	Sn			Sn		
U39	TSOP-50	SnPb		SnCu			SnCu		
U40	TSOP-50	SnPb		SnCu			SnCu		
U41	TQFP-144	SnPb		Sn			Sn		
U42	CSP-100	SnPb		SnAgCu			SnAgCu		
U43	BGA-225	SnPb		SnAgCu			SnAgCu		
U44	BGA-225	SnPb		SnAgCu			SnAgCu		
U45	CLCC-20	SnPb		Sn3.9Ag0.6Cu			Sn3.4Ag1Cu3.3Bi		
U46	CLCC-20	SnPb		Sn3.9Ag0.6Cu			Sn3.4Ag1Cu3.3Bi		
U47	PLCC-20	SnPb		Sn			Sn		
U48	TQFP-208	SnPb		NiPdAu			NiPdAu		
U49	PDIP-20		SnPb	NiPdAu			NiPdAu		
U50	Hybrid-30	SnPb		Sn3.9Ag0.6Cu			Sn3.4Ag1Cu3.3Bi		
U51	PDIP-20		SnPb	Sn			Sn		
U52	CLCC-20	SnPb		Sn3.9Ag0.6Cu			Sn3.4Ag1Cu3.3Bi		
U53	CLCC-20	SnPb		Sn3.9Ag0.6Cu			Sn3.4Ag1Cu3.3Bi		
U54	PLCC-20	SnPb		Sn			Sn		
U55	BGA-225	SnPb		SnAgCu			SnAgCu		
U56	BGA-225	SnPb		SnAgCu			SnAgCu		
U57	TQFP-208	SnPb		NiPdAu	NiPdAu	Sn3.9Ag0.6Cu	NiPdAu	NiPdAu	Sn3.4Ag1Cu3.3Bi
U58	TQFP-144	SnPb		Sn			Sn		
U59	PDIP-20		SnPb	NiPdAu	NiPdAu	Sn3.9Ag0.6Cu	NiPdAu	NiPdAu	Sn0.7Cu0.05Ni
U60	CSP-100	SnPb		SnAgCu			SnAgCu		
U61	TSOP-50	SnPb		SnCu			SnCu		
U62	TSOP-50	SnPb		SnCu			SnCu		
U63	PDIP-20		SnPb	Sn			Sn		

Reworked components are shown in red. Hybrids and CSPs were left off of the test vehicles. SnAgCu BGA balls were Sn4.0Ag0.5Cu.

Originally presented at IPC/JEDEC Global Conference on Lead Free Reliability & Reliability Testing, Boston, MA, April 10-11, 2007. This new version is slightly modified.

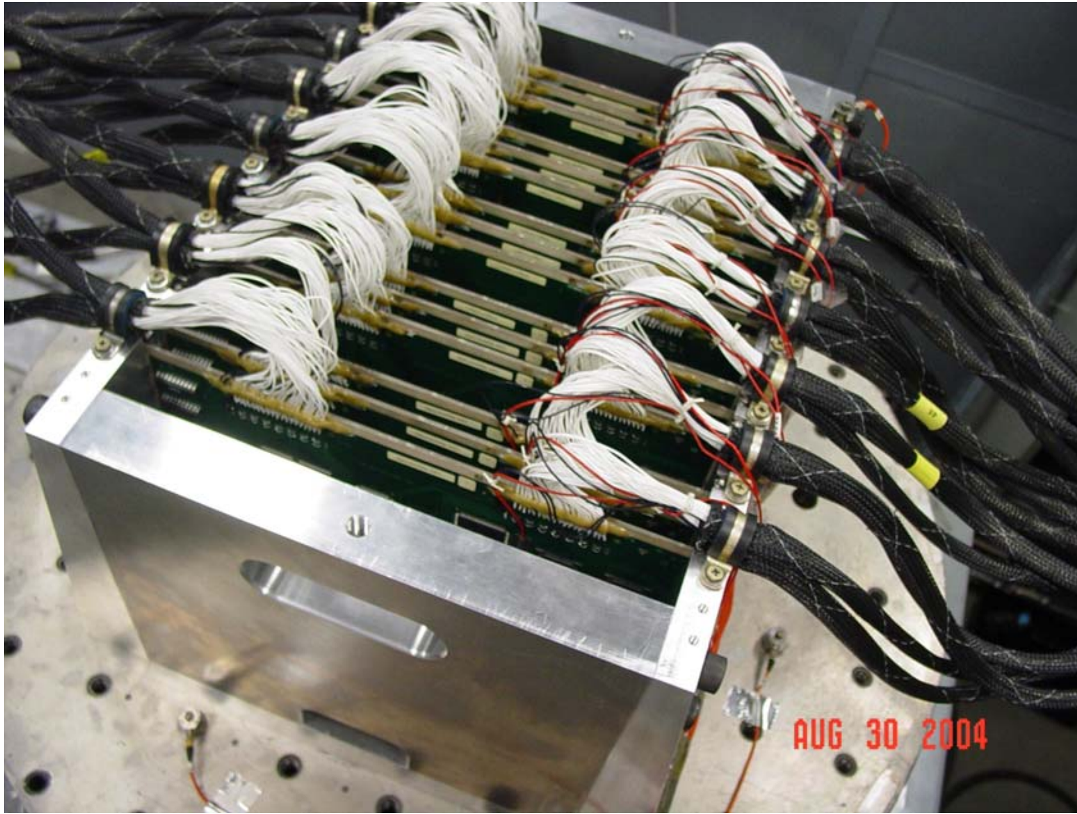

Figure 3. Test Vehicles in Fixture ("Manufactured" Test Vehicles)

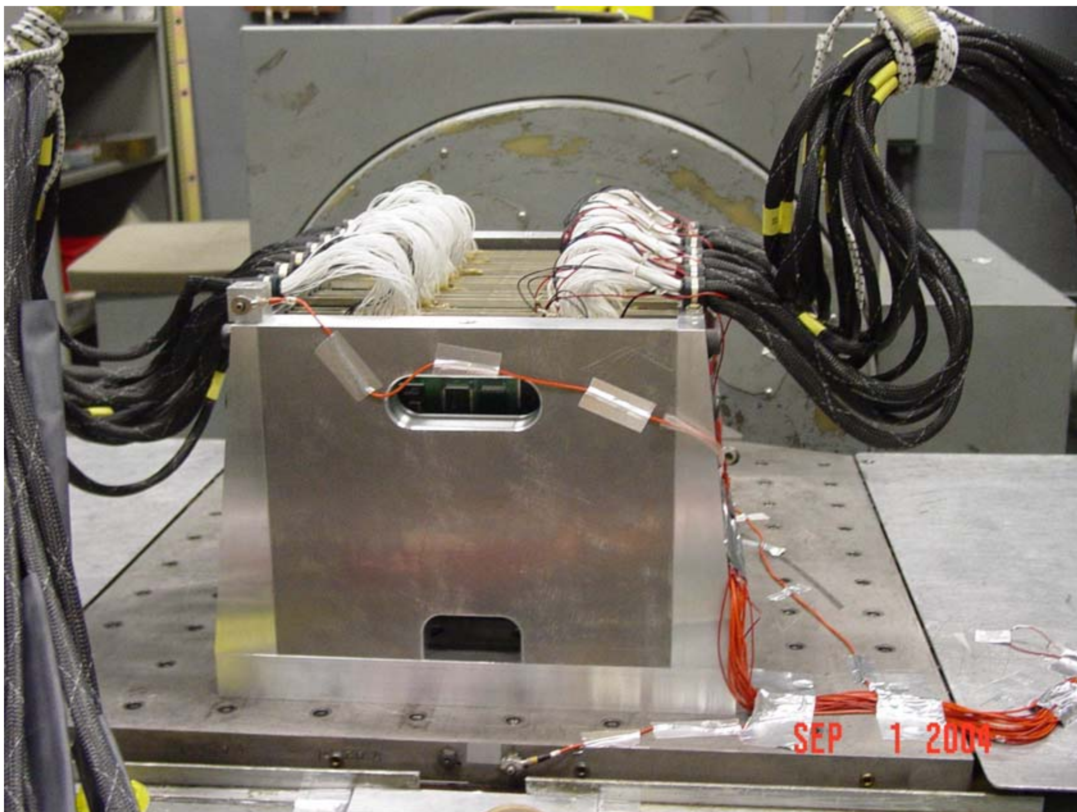

Figure 4. Test Vehicles in Fixture (Z-axis Test)

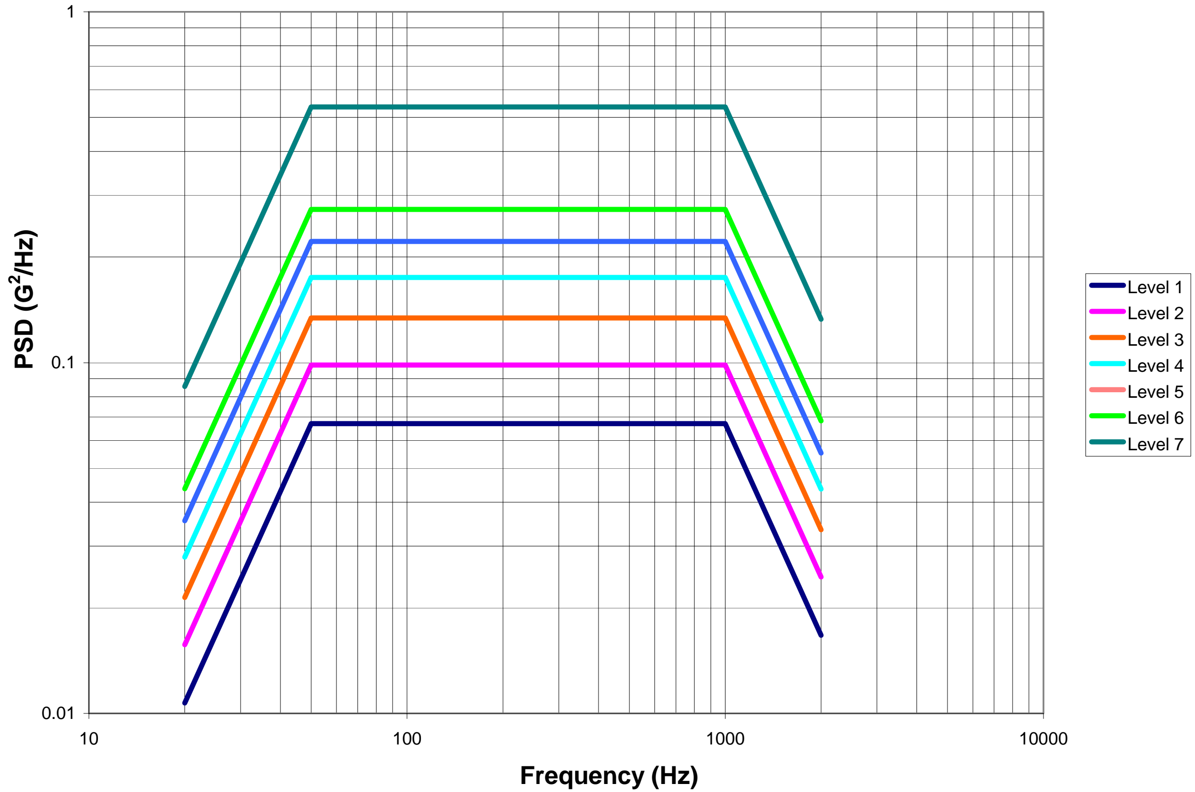

Figure 5. Vibration Test Levels

Table 5. Vibration Test Levels

Level 1	Level 2	Level 3
20 Hz @ 0.0107 G^2/Hz	20 Hz @ 0.0157 G^2/Hz	20 Hz @ 0.0214 G^2/Hz
20 - 50 Hz @ +6.0 dB/octave	20 - 50 Hz @ +6.0 dB/octave	20 - 50 Hz @ +6.0 dB/octave
50 - 1000 Hz @ 0.067 G^2/Hz	50 - 1000 Hz @ 0.0984 G^2/Hz	50 - 1000 Hz @ 0.134 G^2/Hz
1000 - 2000 Hz @ -6.0 dB/octave	1000 - 2000 Hz @ -6.0 dB/octave	1000 - 2000 Hz @ -6.0 dB/octave
2000 Hz @ 0.0167 G^2/Hz	2000 Hz @ 0.0245 G^2/Hz	2000 Hz @ 0.0334 G^2/Hz
Composite = 9.9 G_{rms}	**Composite = 12.0 G_{rms}**	**Composite = 14.0 G_{rms}**

Level 4	Level 5	Level 6
20 Hz @ 0.0279 G^2/Hz	20 Hz @ 0.0354 G^2/Hz	20 Hz @ 0.0437 G^2/Hz
20 - 50 Hz @ +6.0 dB/octave	20 - 50 Hz @ +6.0 dB/octave	20 - 50 Hz @ +6.0 dB/octave
50 - 1000 Hz @ 0.175 G^2/Hz	50 - 1000 Hz @ 0.2215 G^2/Hz	50 - 1000 Hz @ 0.2734 G^2/Hz
1000 - 2000 Hz @ -6.0 dB/octave	1000 - 2000 Hz @ -6.0 dB/octave	1000 - 2000 Hz @ -6.0 dB/octave
2000 Hz @ 0.0436 G^2/Hz	2000 Hz @ 0.0552 G^2/Hz	2000 Hz @ 0.0682 G^2/Hz
Composite = 16.0 G_{rms}	**Composite = 18.0 G_{rms}**	**Composite = 20.0 G_{rms}**

Level 7
20 Hz @ 0.0855 G^2/Hz
20 - 50 Hz @ +6.0 dB/octave
50 - 1000 Hz @ 0.5360 G^2/Hz
1000 - 2000 Hz @ -6.0 dB/octave
2000 Hz @ 0.1330 G^2/Hz
Composite = 28.0 G_{rms}

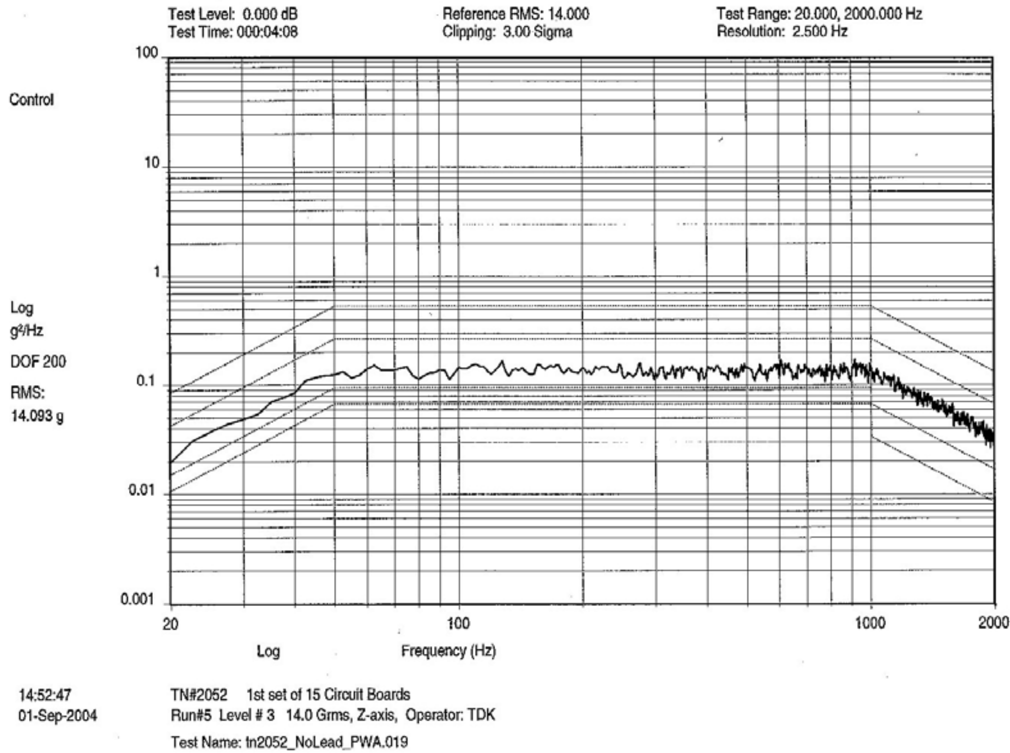

Figure 6. Input (14.0 Grms, Z-axis)

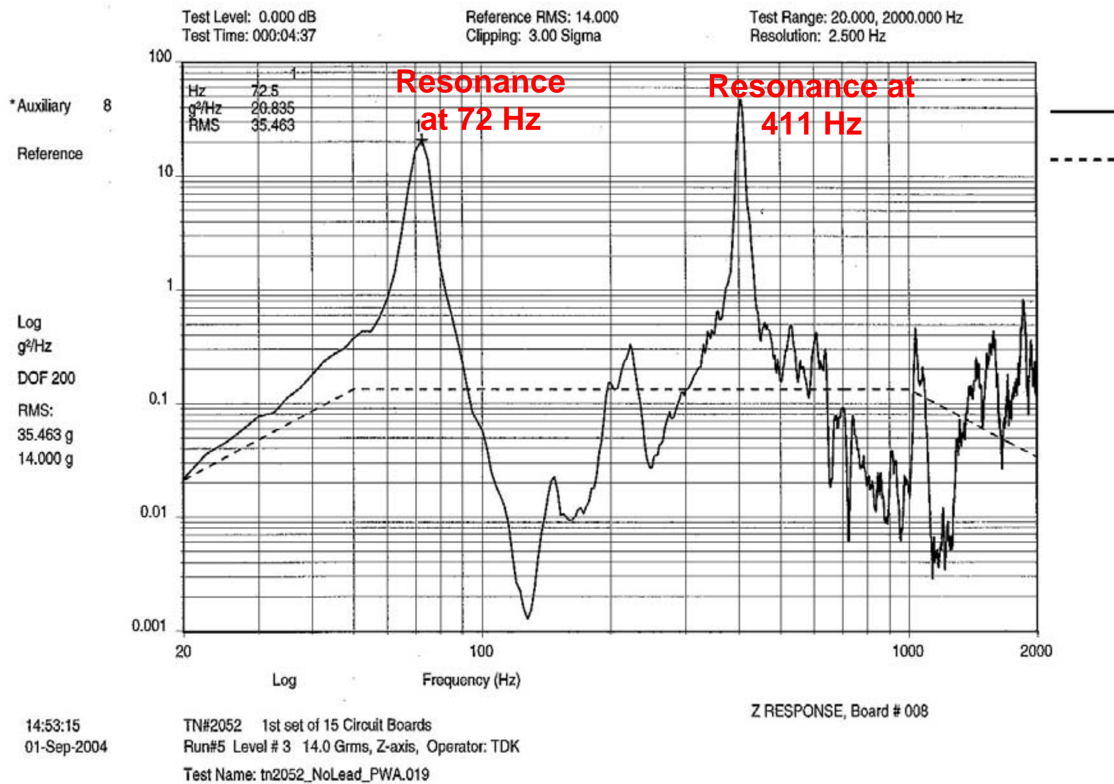

Figure 7. Test Vehicle Response (14.0 Grms, Z-axis, "Manufactured" Test Vehicle 8)

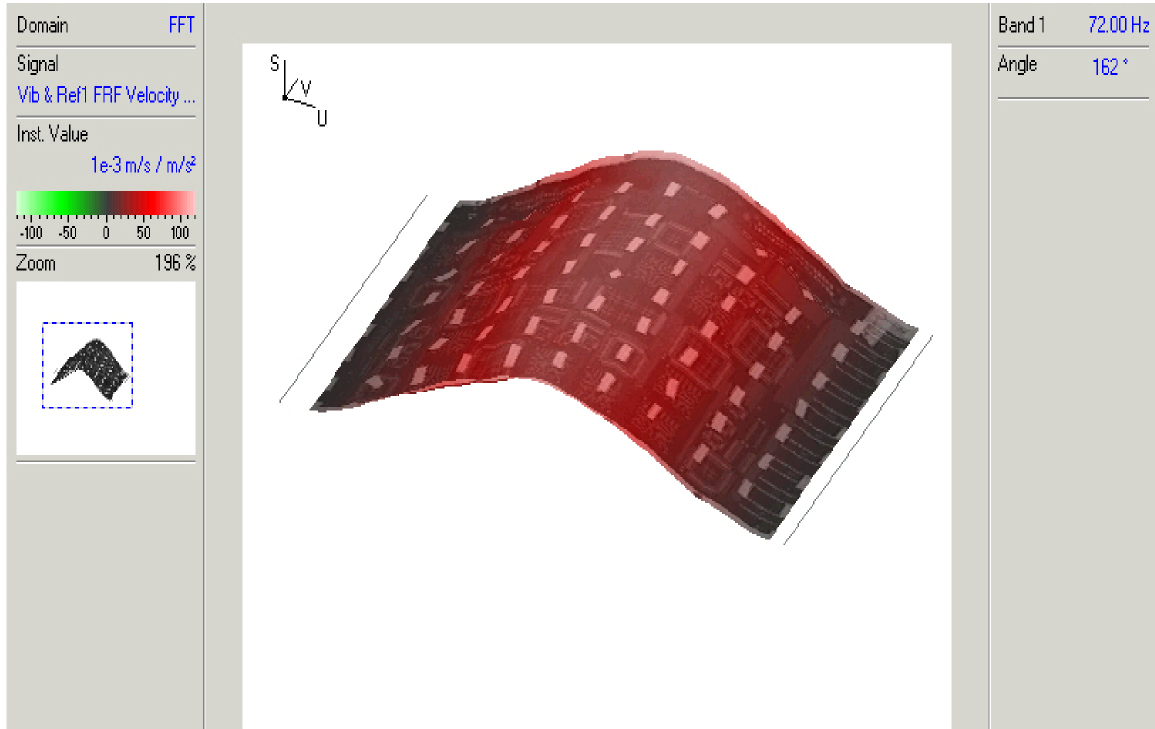

Figure 8. Operating Deflection Shape of Test Vehicle at 72 Hz

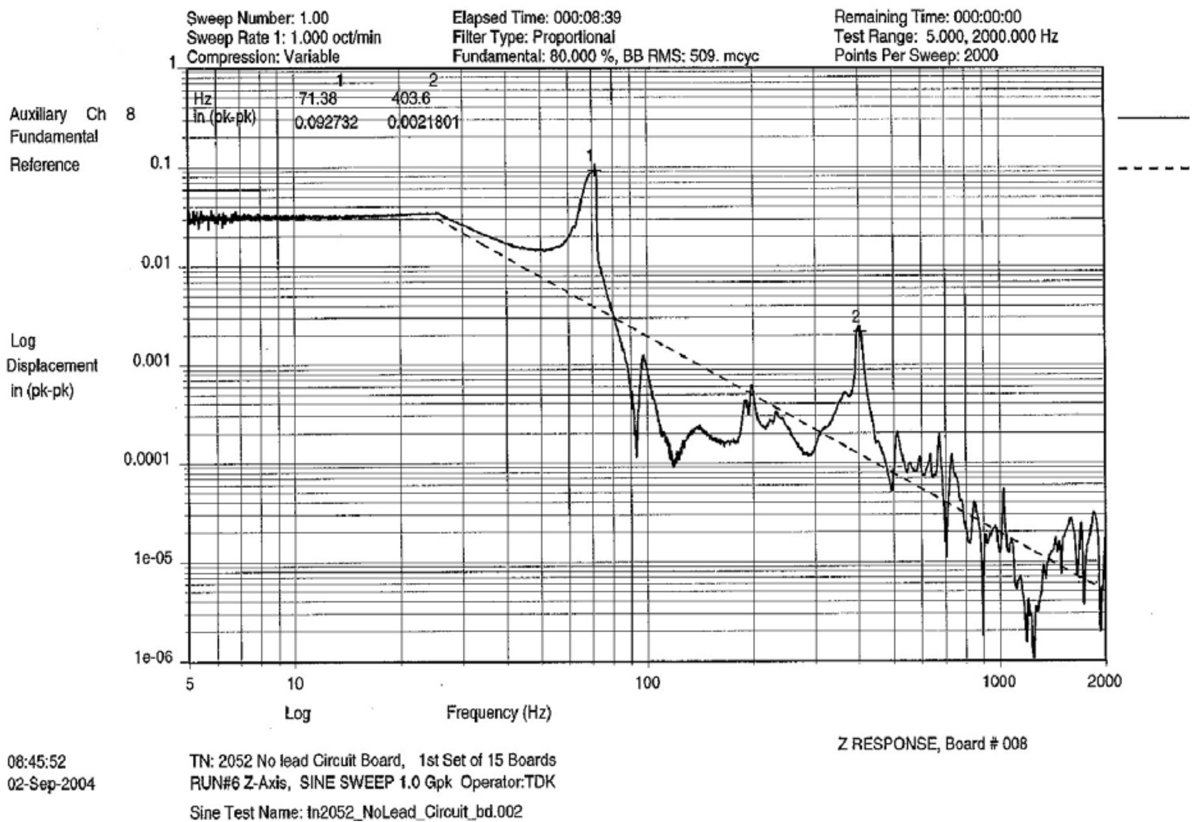

Figure 9. Displacement vs. Frequency ("Manufactured" Test Vehicle 8)

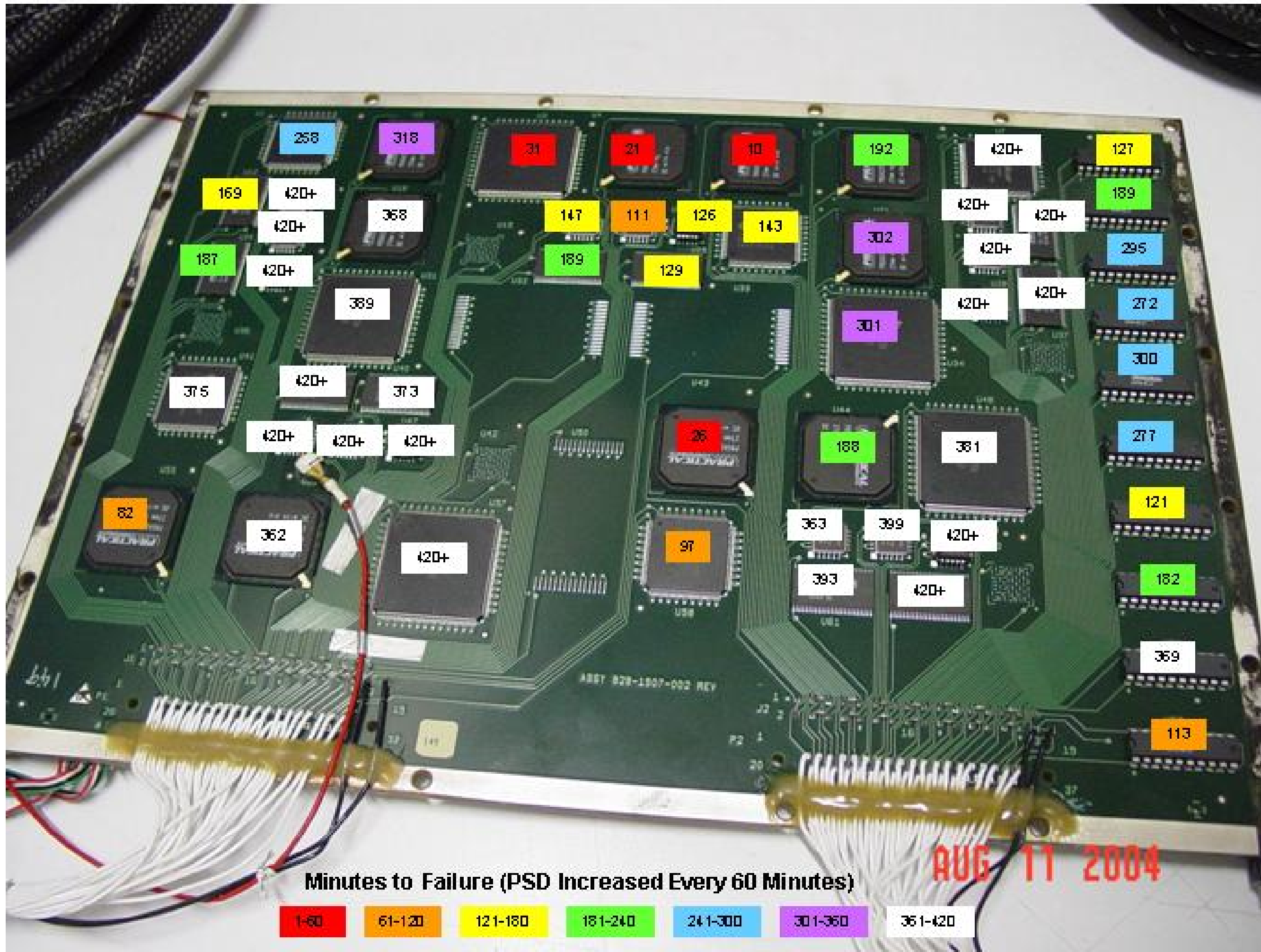

Figure 10. Times to Failure ("Manufactured" Test Vehicle 149)

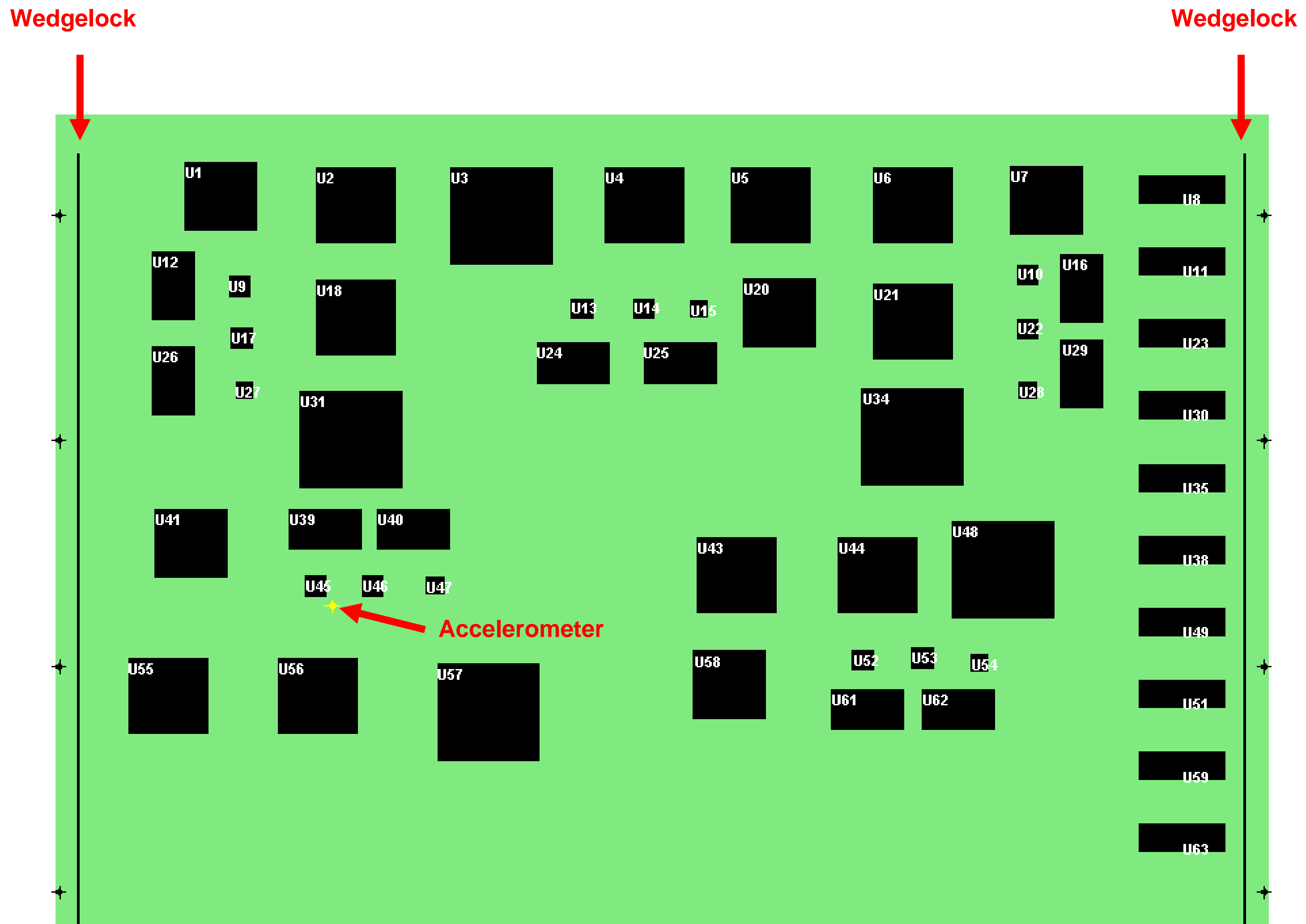

Figure 11. CirVibe Model of JG-PP Test Vehicle

Table 6. Typical Acceleration Factors for JG-PP Test Vehicles

Stress Step Level (Grms)	Test Vehicle 7	Test Vehicle 5
9.9	1	1
12	5.74	6.13
14	16.47	23.66
16	94.82	60.05
18	113.3	94.72
20	339.6	163.0
28	3945	2668

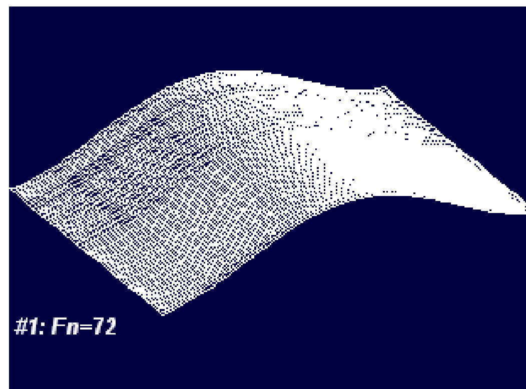

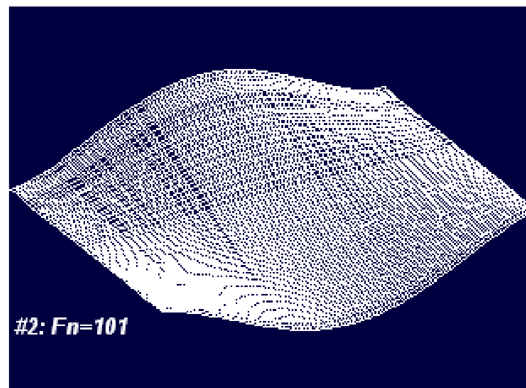

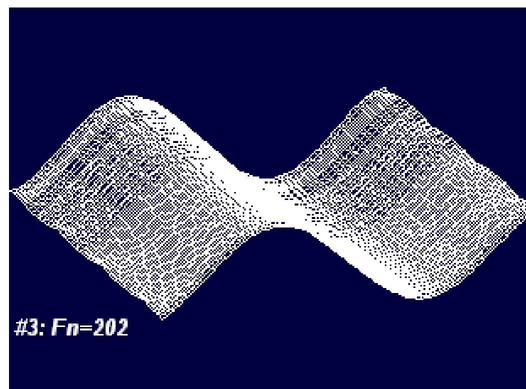

Figure 12. CirVibe Prediction of the First Three Modes of the JG-PP Test Vehicle

Table 7. CirVibe Prediction of the Times to Failure for SnPb BGA's on JG-PP Test Vehicle 5
(Q values at accelerometer for Modes 1, 2 and 3 were 29, 8.5, and 2.6 respectively)

BGAs (Test Vehicle 5, SnPb Solder/SnPb Balls)					
BGA	**Dominant Modes**	**Time to Failure from JG-PP Data (min)**	**Predicted Time to Failure from Model (min)**	**Predicted Time to Failure from Model at Constant 3 Grms Input (years)**	**Predicted Time to Failure from Model at Constant 5 Grms Input (years)**
U4	1	**49**	**49**	14.3	0.09
U5	1	**70**	**62**	35	0.2
U6	2,1	**145**	**145**	297	1.8
U2	2	**195**	**207**	800	4.9
U18	2	**319**	**207**	4145	25
U43	1	**63**	**87**	23	0.14
U44	1	**196**	**155**	818	5
U56	2	**420+**	**304**	52700+	320+
U21	2,1	401	136	37950	230
U55	1	153	13	352	2

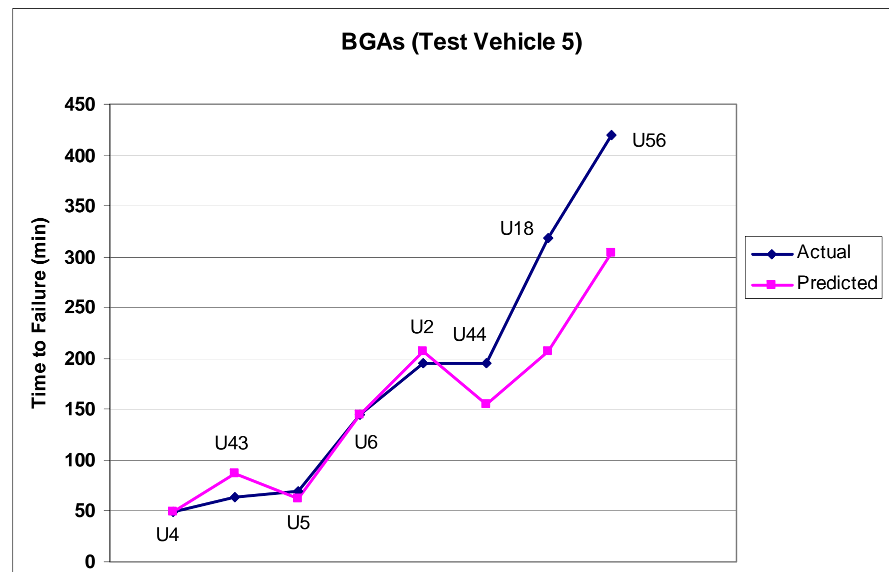

Table 8. CirVibe Prediction of the Times to Failure for SnPb BGA's on JG-PP Test Vehicle 7 (Q values at accelerometer for Modes 1, 2 and 3 were 27.4, 2, and 6.7 respectively)

BGAs (Test Vehicle 7, SnPb Solder/SnPb Balls)					
BGA	Dominant Modes	Time to Failure from JG-PP Data (min)	Predicted Time to Failure from Model (min)	Predicted Time to Failure from Model at Constant 3 Grms Input (years)	Predicted Time to Failure from Model at Constant 5 Grms Input (years)
U4	1	**61**	**61**	19.2	0.12
U5	1	**69**	**66**	33	0.2
U6	1	**330**	**226**	7010	43
U2	1	**354**	**365**	9400	57
U18	1,2	**372**	**369**	23800	144
U43	1	**80**	**69**	51	0.3
U44	1	**199**	**167**	930	5.6
U56	2,1	**383**	**513**	36400	220
U21	1	**199**	**214**	930	5.6
U55	1	200	14	960	5.8

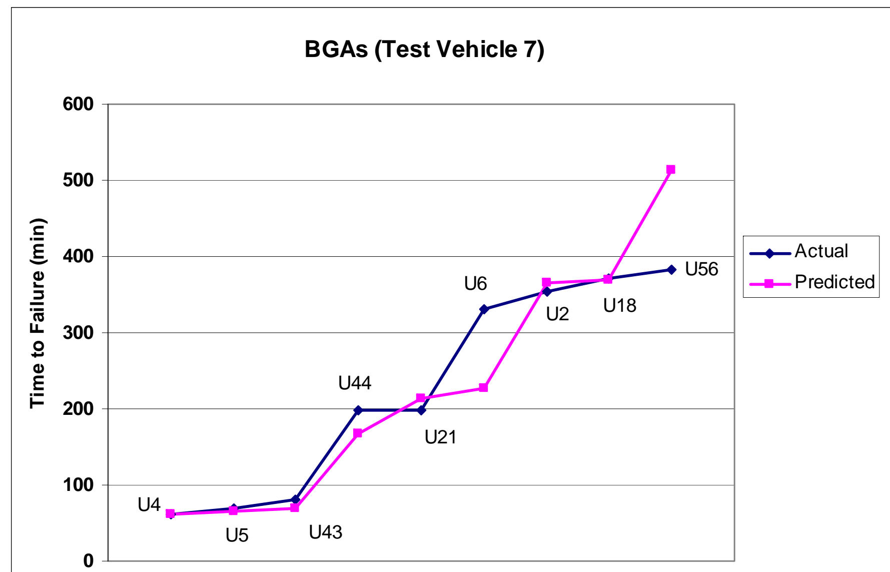

Table 9. CirVibe Prediction of the Times to Failure for SnPb BGA's on JG-PP Test Vehicle 8 (Q values at accelerometer for Modes 1, 2 and 3 were 25, 6, and 4.3 respectively)

BGAs (Test Vehicle 8, SnPb Solder/SnPb Balls)					
BGA	**Dominant Modes**	**Time to Failure from JG-PP Data (min)**	**Predicted Time to Failure from Model (min)**	**Predicted Time to Failure from Model at Constant 3 Grms Input (years)**	**Predicted Time to Failure from Model at Constant 5 Grms Input (years)**
U4	1	**82**	**32**	40	0.2
U5	1	**45**	**45**	13	0.08
U6	1,2	**192**	**191**	330	2
U2	2	**384**	**251**	16550	100
U18	2	**420+**	**253**	35850+	217+
U43	1	**76**	**76**	34	0.2
U44	1	**188**	**166**	301	1.8
U56	2	**404**	**352**	22270	165
U21	2,1	420+	181	35850+	217+
U55	1	78	8	36	0.2

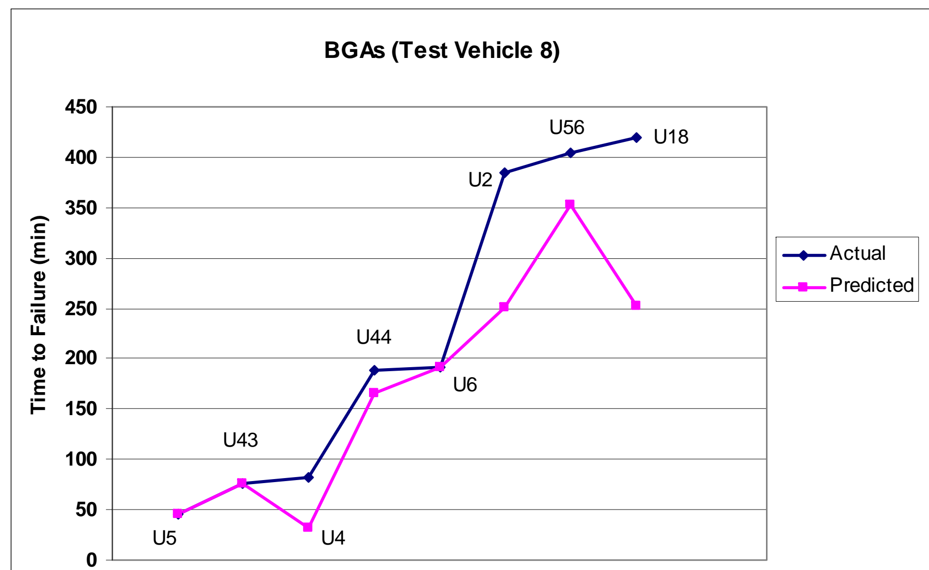

Table 10. CirVibe Prediction of the Times to Failure for SAC BGA's on JG-PP Test Vehicle 75 (Q values at accelerometer for Modes 1, 2 and 3 were 22.3, 5, and 4 respectively)

BGAs (Test Vehicle 75, SAC Solder/SAC Balls)					
BGA	Dominant Modes	Time to Failure from JG-PP Data (min)	Predicted Time to Failure from Model (min)	Predicted Time to Failure from Model at Constant 3 Grms Input (years)	Predicted Time to Failure from Model at Constant 5 Grms Input (years)
U4	1	10	10	0.93	0.009
U6	1,2	151	124	47	0.46
U18	2	380	173	2430	24.0
U55	1	8	3	0.75	0.007
U43	1	10	30	0.93	0.009

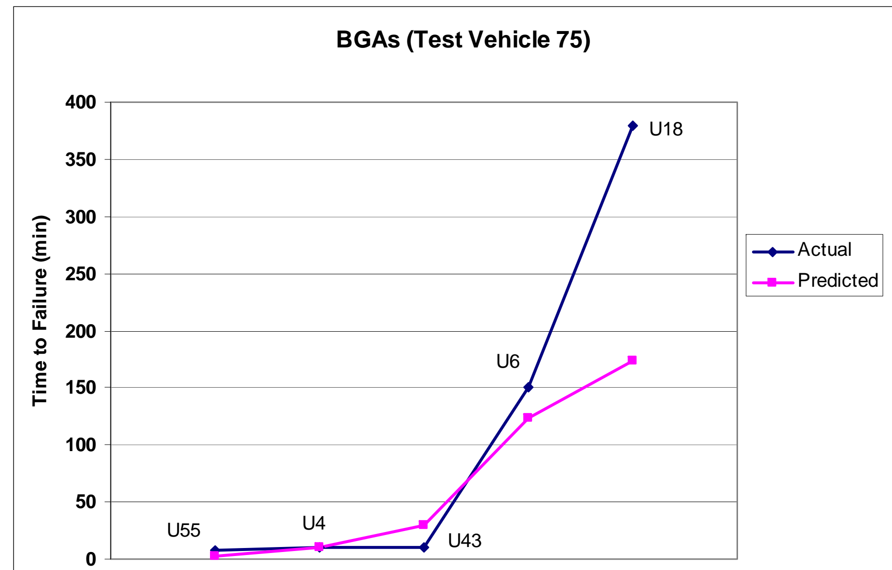

Table 11. CirVibe Prediction of the Times to Failure for SAC BGA's on JG-PP Test Vehicle 77 (Q values at accelerometer for Modes 1, 2 and 3 were 22.6, 8.6, and 7 respectively)

BGAs (Test Vehicle 77, SAC Solder/SAC Balls)					
BGA	**Dominant Modes**	**Time to Failure from JG-PP Data (min)**	**Predicted Time to Failure from Model (min)**	**Predicted Time to Failure from Model at Constant 3 Grms Input (years)**	**Predicted Time to Failure from Model at Constant 5 Grms Input (years)**
U4	1	**6**	**17**	0.56	0.006
U6	2	**84**	**84**	13	0.13
U18	2	**202**	**134**	104	1.0
U55	1	**11**	**5**	1.0	0.01
U43	1	6	68	0.6	0.006

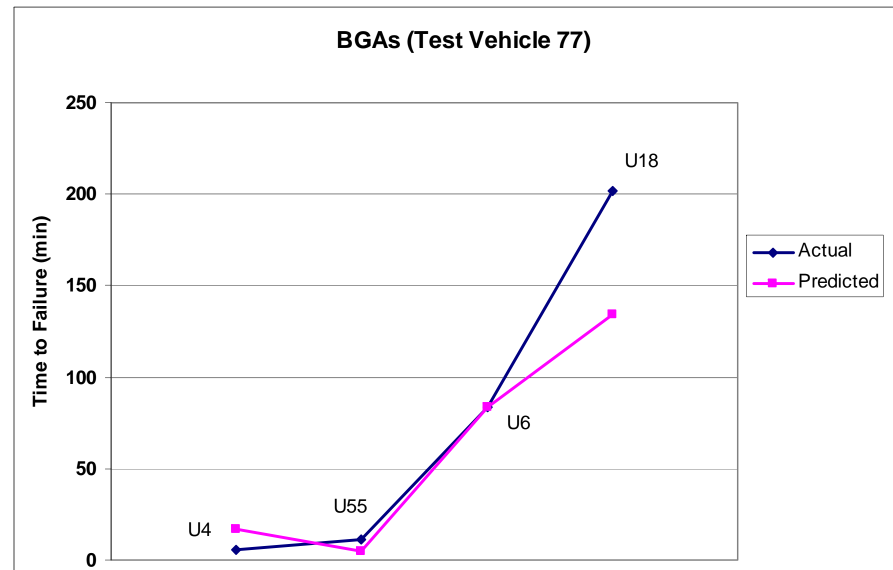

Table 12. Comparison of Predicted Times to Failure for SnPb and SAC BGA's

	Predicted Time to Failure at Constant 3 Grms (0.0062 G^2/Hz) Input (years)					
BGA	**Test Vehicle 5, SnPb Solder**	**Test Vehicle 7, SnPb Solder**	**Test Vehicle 8, SnPb Solder**	**Test Vehicle 75, SAC Solder**	**Test Vehicle 77, SAC Solder**	**Test Vehicle 79, SAC Solder**
U4	14.3	19.2	40	0.9	0.6	0.8
U6	297	7010	330	47	13.3	1.6
U18	4145	23800	35850+	2430	102	228